DOI: 10.31534/engmod.2025.2.ri.05f
Original scientific paper
Received: 15.09.2025.

Thermoelastic Effect in a Large Lubricated Thrust Bearing

Yansun Zhou

School of Electrical Engineering, Jiangxi Metallurgical Vocational and Technical College, Xinyu, CHINA
e-mail: sheldorbko@sina.com

SUMMARY

The numerical simulation results are presented for the performance of a large lubricated thrust bearing, considering surface elasticity and surface thermal distortion under large loads and high sliding speeds. The bearing shaft and bush are respectively made of steel and bronze. The results show that the film thickness and film pressure profiles were largely changed by the surface thermal distortion. Due to the surface thermoelastic effect, a large load results in a minimum lubricating film thickness that is far smaller than that predicted by conventional hydrodynamic lubrication theory calculation, and the minimum film thickness is much more sensitive to load variation than predicted by conventional hydrodynamic lubrication theory description. The minimum film thickness does not vary with an increase of the sliding speed when the sliding speed is sufficiently high. The effect of the adsorbed layer considerably increases the minimum film thickness, which is below 100 nm, particularly in the case of strong fluid-bearing interaction.

KEY WORDS: *adsorbed molecule; film pressure; film thickness; thermoelastic deformation; thrust bearing.*

1. INTRODUCTION

Large hydrodynamic lubricated thrust bearings are widely applied in large mechanical equipment for supporting large axial loads and reducing friction and wear [1-9]. Good lubrication is critical for maintaining the performance of these bearings. However, in practice these bearings face the risk of lubricant film breakdown and pad seizure [10-12]. Such phenomena are difficult to explain using conventional hydrodynamic lubrication theory [13], which predicts that there are much thicker lubricate films in these bearings. Furthermore, the effects of fluid non-Newtonian shear thinning, surface roughness and lubricant viscosity reduction due to film viscous heating are not responsible for the film breakdown [14-16]. This behavior has been attributed to thermoelastic deformation of the thermoelastic deformation of the bearing [10-12].

Before pad seizure, there is a lubrication stage in the bearing during which the fluid film thickness is very low, so that the influence of the fluid molecule layer physically adsorbed onto the bearing surface should be considered. To date, few studies have investigated bearing

performance at this stage, except for the work of Ye and Zhang, who presented the results for the step bearing [17].

This paper investigates this previously unexplored lubrication stage before film breakdown in a large-sized inclined fixed pad thrust bearing by considering both surface thermoelastic deformation and the physically adsorbed molecule layer. unlike the study of Ye and Zhang [17], the coupled shaft and bush surfaces of the bearing are made of steel and bronze, respectively. Different fluid-surface interactions are considered, and calculation results are presented for various parameter values. These results provide a new understanding of the lubrication behavior of this large thrust bearing.

2. LARGE HYDRODYNAMIC LUBRICATED INCLINED FIXED PAD THRUST BEARING WITH THERMAL DISTORTION

The large hydrodynamic lubricated inclined fixed pad thrust bearing investigated in this study is shown in Figure 1. Because of surface thermal distortion, the bearing clearance profile is significantly different from that predicted by conventional theory. Under condition of very small film thicknesses, the ultrathin adsorbed molecule layer becomes significant. Although the lower shaft surface is moving and made of steel and the upper bush surface is stationary and made of bronze, the two adsorbed layers do not differ because of the same coatings applied to both surfaces. Moreover, by using different coatings, the fluid-surface interaction can be altered.

Here, u is the sliding speed, $h_{tot,i}$ and $h_{tot,o}$ are the surface separations at the bearing **inlet and outlet**, respectively; h_{bf} is the thickness of the adsorbed molecular layer; h is the thickness of the continuum fluid film; h_o is the value of h on the bearing outlet; l is the bearing width; and the coordinate system is also illustrated.

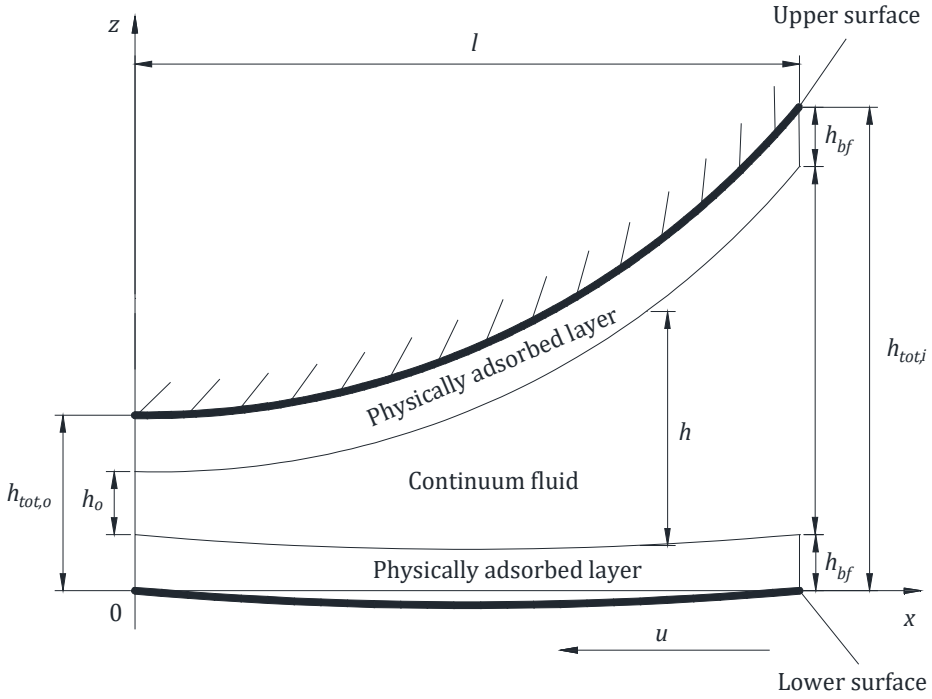

Fig. 1 *Large hydrodynamic lubricated inclined fixed-pad thrust bearing under thermal distortion investigated in this study*

3. THEORETICAL ANALYSIS AND NUMERICAL CALCULATION

To perform the numerical calculations for the multiscale flow problem in the bearing, Zhang's multiscale flow model [18] was used, rather than the classical hybrid schemes [19-21]. The following assumptions were adopted:

(1) The lubricant is Newtonian;

(2) The surface has no roughness;

(3) Film slippage is absent;

(4) The lubricant side flow is absent;

(5) The loading is steady.

At high sliding speeds, the fluid in the bearing may be non-Newtonian, and the interfacial slippage may occur. In addition, for very small film thicknesses, the surface roughness effect may become significant. Assumptions (1)-(3) allow this study to focus on the combined effects of the physically adsorbed layer and surface thermal distortion. The effects of lubricant non-Newtonian shear thinning, surface roughness and lubricant side leakage are not expected to alter the conclusions presented here. A new model would be required to simulatenon-Newtonian fluid behavior and side - flow effects.

Based on the above assumptions, the total mass flow rate per unit contact length through the bearing is given by [17, 18]:

$$\begin{aligned} q_m = & -uh_{bf}\rho_{bf}^{eff} - \frac{uh}{2}\rho - \frac{h^3\rho}{12\eta}\frac{\partial p}{\partial x} \\ & + \frac{h_{bf}^3\rho_{bf}^{eff}}{\eta_{bf}^{eff}}\frac{\partial p}{\partial x}\left[\frac{F_1}{6} - \frac{\varepsilon}{1+\frac{\Delta x}{D}}\left(1+\frac{1}{2\lambda_{bf}} - \frac{q_o - q_o^n}{q_o^{n-1} - q_o^n}\frac{\Delta_{n-2}}{h_{bf}}\right)\right] \\ & + \frac{h^3\rho}{\eta_{bf}^{eff}}\frac{\partial p}{\partial x}\left[\frac{F_2\lambda_{bf}^2}{6} - \frac{\lambda_{bf}}{1+\frac{\Delta x}{D}}\left(\frac{1}{2}+\lambda_{bf} - \frac{q_o - q_o^n}{q_o^{n-1} - q_o^n}\frac{\Delta_{n-2}}{h}\right)\right] \end{aligned} \tag{1}$$

where the definitions of the parameters are given by Ye and Zhang [17].

Defining $C_y = \eta_{bf}^{eff} / \eta$, according to Eq. (1) the pressure gradient is:

$$\frac{dp}{dx} = \frac{\frac{1}{2}u\rho h + q_m + uh_{bf}\rho_{bf}^{eff}}{\frac{c\rho h^3}{\eta} + \frac{d\rho_{bf}^{eff}h_{bf}^3}{\eta_{bf}^{eff}}} \tag{2}$$

where:

$$c = \frac{1}{C_y}\left[\frac{F_2\lambda_{bf}^2}{6} - \frac{\lambda_{bf}}{1+\frac{\Delta x}{D}}\left(\frac{1}{2}+\lambda_{bf} - \frac{q_0 - q_0^n}{q_0^{n-1} - q_0^n}\frac{\Delta_{n-2}\lambda_{bf}}{h_{bf}}\right)\right] - \frac{1}{12} \tag{3}$$

$$d = \frac{F_1}{6} - \frac{\varepsilon}{1+\frac{\Delta x}{D}}\left(1+\frac{1}{2\lambda_{bf}} - \frac{q_0 - q_0^n}{q_0^{n-1} - q_0^n}\frac{\Delta_{n-2}}{h_{bf}}\right) \tag{4}$$

The thickness of the adsorbed layer is given by:

$$h_{bf} = nD + \Delta_{n-2}\frac{q_0 - q_0^n}{q_0^{n-1} - q_0^n} \tag{5}$$

The thickness of the continuum fluid film is expressed as:

$$h(x) = h_{00} + f(x) - \frac{2}{\pi E_v}\int_0^l p(s)\ln(x-s)^2 ds + \frac{x^2}{2R_t} - 2h_{bf} \tag{6}$$

where h_{oo} is constant, p is the film pressure, E_v is the equivalent of Young's modulus of elasticity of the two bearing surfaces, and:

$$f(x) = x\tan\theta \tag{7}$$

Here, θ is the tilting angle of the original geometrical shape of the bearing, R_t is defined in [22]:

$$R_t = \frac{R_{t,a}R_{t,b}}{R_{t,a} + R_{t,b}} \tag{8}$$

$R_{t,a}$ and $R_{t,b}$ are, respectively [22]:

$$R_{t,a} = \frac{k_a\rho_a c_a}{u\lambda_a\tau_{av}\alpha_a(1+\nu_a)(1-\chi)} \tag{9}$$

$$R_{t,b} = \frac{k_b\rho_b c_b}{u\lambda_b\tau_{av}\alpha_b(1+\nu_b)(1-\chi)} \tag{10}$$

k denotes the surface thermal diffusivity, c the surface specific heat, ρ the surface density, v the surface Poisson's ratio, α the surface linear thermal expansion coefficient, λ the frictional heat input rate into the surface, χ the rate of the frictional heating removed by the lubricant flow, the subscripts "a" and "b" denote the stationary and moving surfaces, respectively, and τ_{av} represents the average shear stresses on each surfaces which is calculated as:

$$\tau_{av} = \frac{w(f_a + f_b)}{2l} \tag{11}$$

w denotes the bearing load per unit contact length, f_a, f_b are the friction coefficients on the stationary and moving surfaces, respectively. The effect of surface roughness can be studied using the present model only if a term accounting for surface roughness is added to Eq. (6).

The surface shear stresses at the j^{th} discretized point are given by [17]:

$$\tau_{a,j} = \eta\frac{\bar{u}_a - \bar{u}_b}{\frac{2\Delta_{n-2}\left[q_0^{(1+\gamma)} - q_0^{-(n-2)(1+\gamma)}\right]}{q_0^{(1+\gamma)} - 1} + h_j} + \left.\frac{dp}{dx}\right|_j\left(\frac{h_j}{2} + Dn - D\right) \tag{12}$$

$$\tau_{b,j} = \eta\frac{\bar{u}_a - \bar{u}_b}{\frac{2\Delta_{n-2}\left[q_0^{(1+\gamma)} - q_0^{-(n-2)(1+\gamma)}\right]}{q_0^{(1+\gamma)} - 1} + h_j} - \left.\frac{dp}{dx}\right|_j\left(\frac{h_j}{2} + Dn - D\right) \tag{13}$$

The pressure gradient is:

$$\left.\frac{dp}{dx}\right|_j = \frac{p_j - p_{j-1}}{\delta_x} \quad for\ j = 1,2,\ldots,N \tag{14}$$

where δ_x is the distance between the neighboring discretized points.

According to Eqs. (2) and (14), the film pressure on the j^{th} discretized point is:

$$p_j = p_0 + \delta_x \sum_{i=1}^{j} \frac{\frac{1}{2} u\rho h_i + q_m + u h_{bf} \rho_{bf}^{eff}}{\frac{c\rho h_i^3}{\eta} + \frac{d\rho_{bf}^{eff} h_{bf}^3}{\eta_{bf}^{eff}}} \quad for\, j = 1,\ 2,\ldots,\ N \tag{15}$$

Since $p_0=0$, the bearing load is:

$$w = \int_0^l p dx \tag{16}$$

The surface frictional forces per unit contact length are, respectively:

$$F_a = \int_0^l \tau_{a,j} dx \tag{17}$$

$$F_b = \int_0^l \tau_{b,j} dx \tag{18}$$

The surface friction coefficients are respectively:

$$f_a = \frac{|F_a|}{w},\ f_b = \frac{|F_b|}{w} \tag{19}$$

Here, the solution can only be obtained numerically. The numerical procedure follows that presented by Ye and Zhang [17] and, for conciseness, is not repeated here.

It was defined that $C_q = \rho_{bf}^{eff} / \rho$ [22]. C_q and C_y were formulated in Ref. [22]. F_1, F_2 and ε were regressed out in Ref. [18]. The values of the parameters for different fluid-surface interactions are provided in Ref. [22]. The type of fluid-surface interaction is determined by strength of the interaction between the fluid molecules and the coating molecule on the solid surface. For example, a hydrophobic surface coating produces a weak fluid-surface interaction, a strongly hydrophilic coating produces a strong fluid-surface interaction, and a normally hydrophilic coating may produce a medium fluid-surface interaction. Different fluid-surface interactions lead to variations in local viscosity and density across the adsorbed molecular layer thickness, as well as different discontinuities and non-continuum effects within the adsorbed molecule layer. Definitions of weak, medium, and strong fluid-surface interactions used in this study are given in Ref. [23]. Table 1 shows the input operational parameter values, and Table 2 provides the material property data of the bearing.

Table 1 *Operational parameter values*

Parameter	*Value*
N	*2500*
D	*0.5 nm*
$\Delta x/D$, $\Delta_{n\text{-}2}/D$	*0.15*
E_v	*148 GPa*
η	*0.0035 Pa s*
l	*0.6 m*
ϑ	*0.0001*
χ	*0*

Table 2 *Material properties of the bearing*

Parameter	*Shaft*	*Bush*
Thermal diffusivity: k (m^2/s)	*1.82×10^{-5}*	*1.39×10^{-5}*
Density: ρ (kg/m^3)	*8600*	*7800*
Specific heat: c ($J/kg\ ^oC$)	*360*	*400*
Linear thermal expansion coefficient: α (/K)	*1.7×10^{-5}*	*1.3×10^{-5}*
Poisson ratio: υ	*0.3*	*0.3*
Frictional heat input rate: λ	*0.55*	*0.45*

4. RESULTS AND DISCUSSION

4.1 MINIMUM FILM THICKNESS

Figure 2 shows that, when the surface thermoelastic effect is incorporated, for w=5000 kN/m, the minimum bearing clearance $h_{tot,min}$ increases rapidly with the sliding speed u when is below 40 m/s. With a further increase in speed, the slope of the variation slope of $h_{tot,min}$ with u is significantly reduced. When u exceeds approximately 70 m/s, $h_{tot,min}$ slightly decreases with increasing u. Stronger fluid-surface interactions result in a slightly higher values of $h_{tot,min,}$ even when $h_{tot,min}$=0.5 μm. Figure 3 shows that, for w=5000 kN/m and weak fluid-surface interaction (i.e. the nearly negligible adsorbed layer effect), for the elastic surface without thermal deformation, the calculated $h_{tot,min}$ is slightly smaller than that predicted by classical lubrication theory calculation [13]; however, its variation with u follows the classical hydrodynamic theory. For the elastic surface with thermal deformation, the calculated $h_{tot,min}$ is much lower than the classical theory prediction, and its variation with u does not follow conventional expectations; that is, very high sliding speeds are determinal to bearing lubrication.

Figure 4 shows that for u=40 m/s and the strong fluid-surface interaction, for the elastic surface without thermal deformation, the sensitivity of $h_{tot,min}$ to load variation w is slightly higher than predicted by conventional theory. However, for the elastic surface with thermal deformation, the sensitivity of $h_{tot,min}$ to the variation w is much greater; this indicates that the film stiffness is considerably lower than classical predictions and the bearing load performance is actually significantly worse due to the surface thermoelastic deformation at large loads and high sliding speeds. Figure 5 shows that, when $h_{tot,min}$ is below 0.1 μm, the effect of the adsorbed layer becomes pronounced, and is particularly strong for $h_{tot,min}\leq$0.01 μm. Strong fluid-surface interactions generate a substantially thicker lubricating film when $h_{tot,min}$ is on the 1 nm scale. To improve bearing performance, strong interfacial adsorption on the bearing surface is required, which can be achieved by applying a special coating (strongly hydrophilic or strongly oil-philic) on the bearing surface.

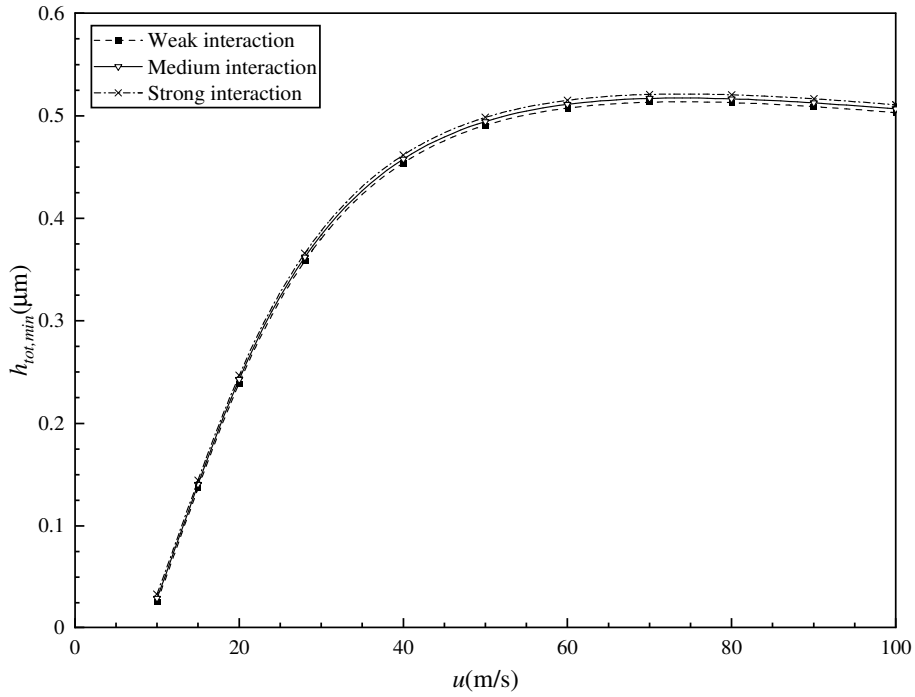

Fig. 2 *Minimum bearing clearance ($h_{tot,min}$) versus sliding speed (u) curves for different fluid–surface interactions at w=5000 kN/m*

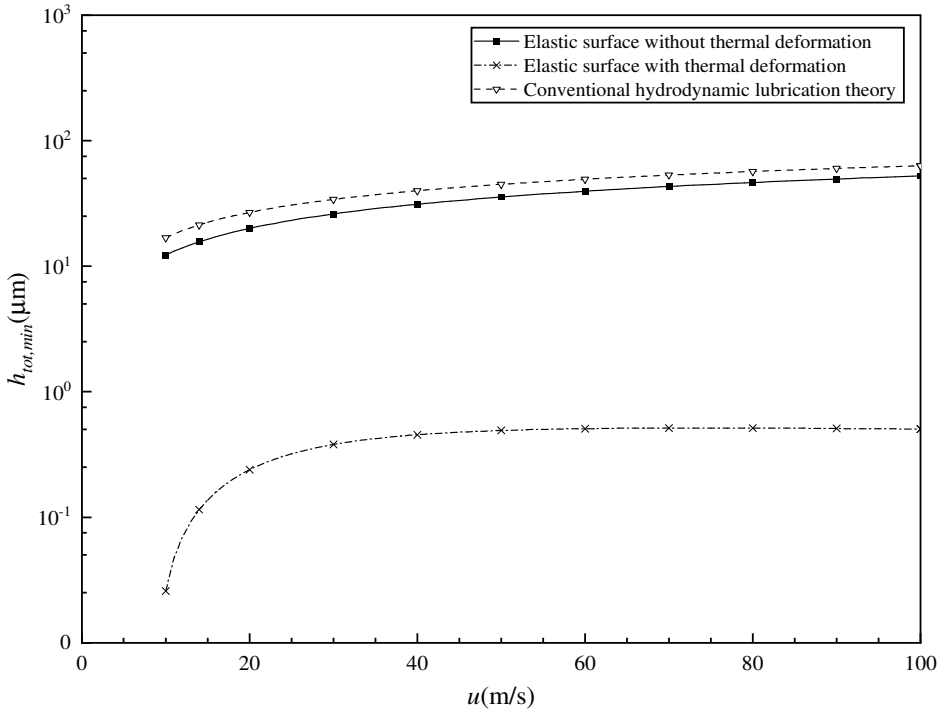

Fig. 3 *Minimum bearing clearance ($h_{tot,min}$) versus sliding speed (u) curves for different contact regimes at w=5000 kN/m with weak fluid-surface interaction*

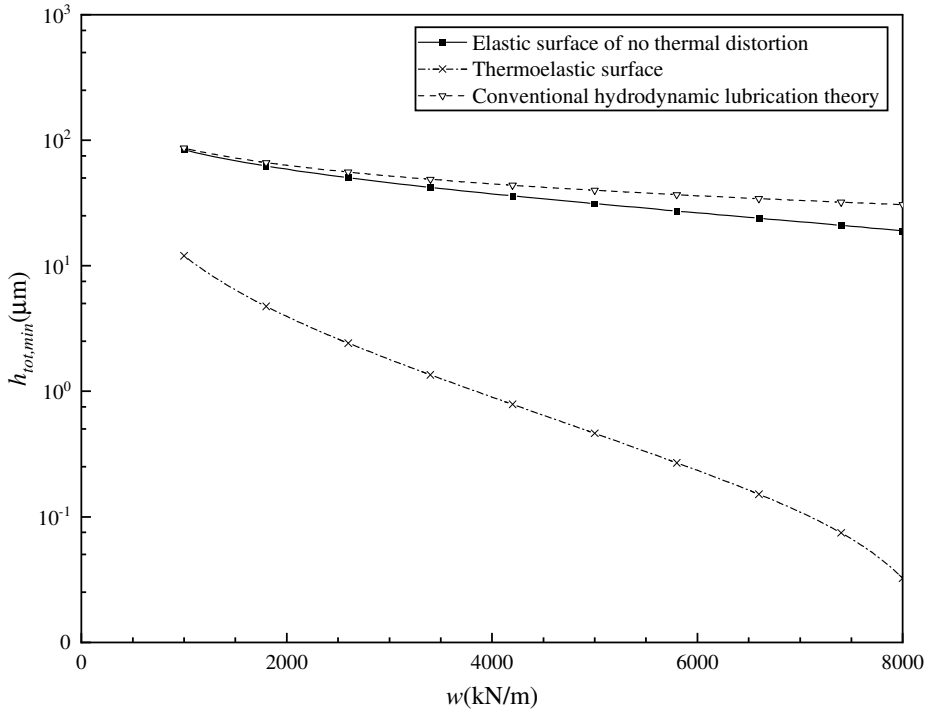

Fig. 4 *Minimum bearing clearance ($h_{tot,min}$) versus load (w) curves for different surfaces at u=40 m/s with strong fluid-surface interaction*

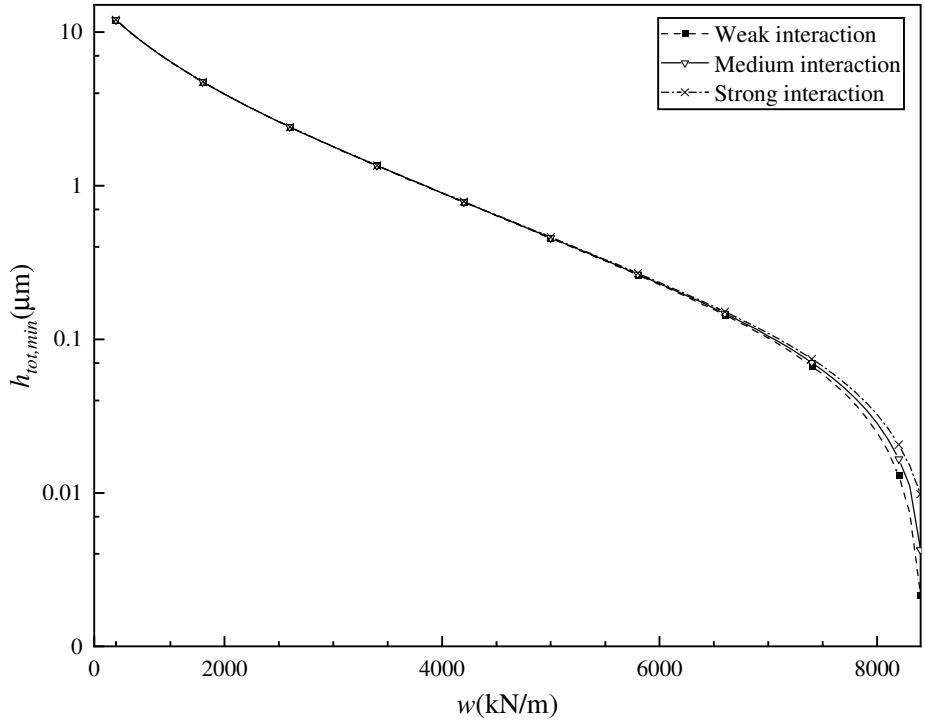

Fig. 5 *Minimum bearing clearance ($h_{tot,min}$) versus load (w) curves for different fluid–surface interfaces at u=40 m/s with thermoelastic surface*

4.2 FILM PRESSURE AND FILM THICKNESS DISTRIBUTIONS

Figures 6(a) and (b) show that surface thermal distortion significantly alters the film pressure profile at large loads and high sliding speeds. Due to surface thermal distortion, as the load increases, the film pressure is reduced across most of the lubricated area, while only in localized narrow regions does the film pressures increase sharply. This behavior deviates from predictions of classical hydrodynamic lubrication theory. Figures 7(a) and (b) show that surface thermal distortion also significantly alters the film thickness distribution at large loads and high sliding speeds. Although the surface thermoelastic effect does not change the location of the minimum bearing clearance, it shifts the location of the maximum film thickness toward the bearing entrance. Due to the surface thermoelastic effect, as the load increases, the film thickness increases across most of the lubricated area, while it decreases sharplyin localized narrow regions. Figure 7(b) corresponds closely to Figure 6(b). The bearing lubrication performance, therefore, deviates from classical hydrodynamic lubrication theory under severe surface thermal distortion. Moreover, Figure 7(b) highlights the practical necessity of cooling large hydrodynamic lubricated thrust bearing, operating under heavy loads and high sliding speeds in order to mitigate the significant effects of surface thermoelastic deformation.

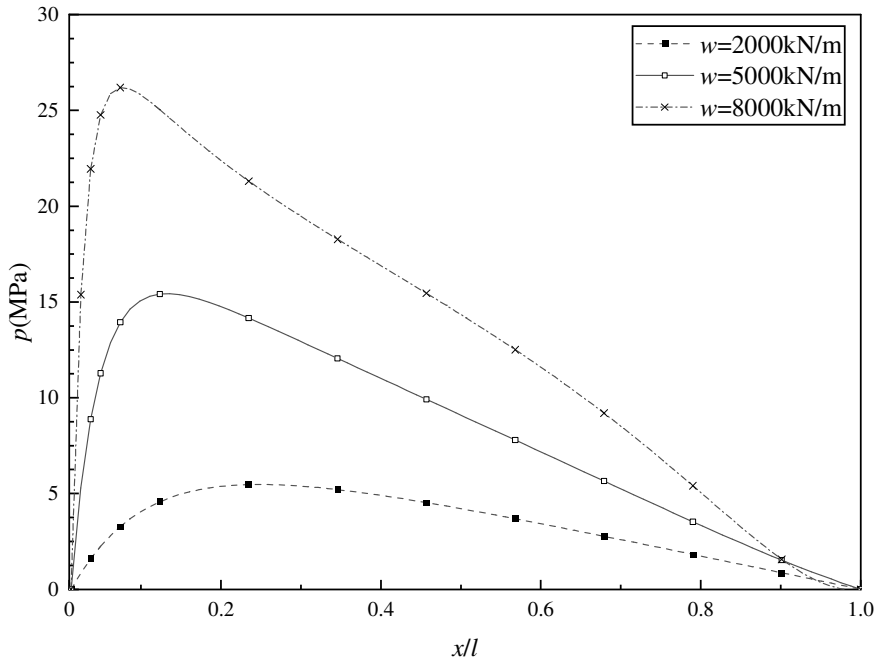

(a) *For elastically deformed surfaces without thermal deformation*

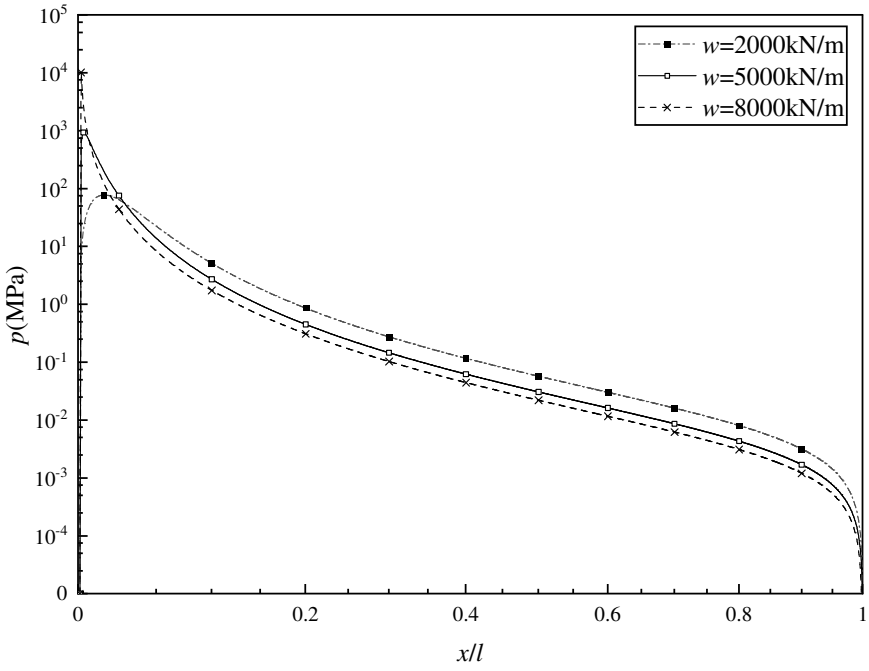

(b) *For elastically deformed surfaces with thermal deformation*

Fig. 6 *Film pressure distributions for different loads and contact regimes at u=40 m/s with medium fluid-surface interaction*

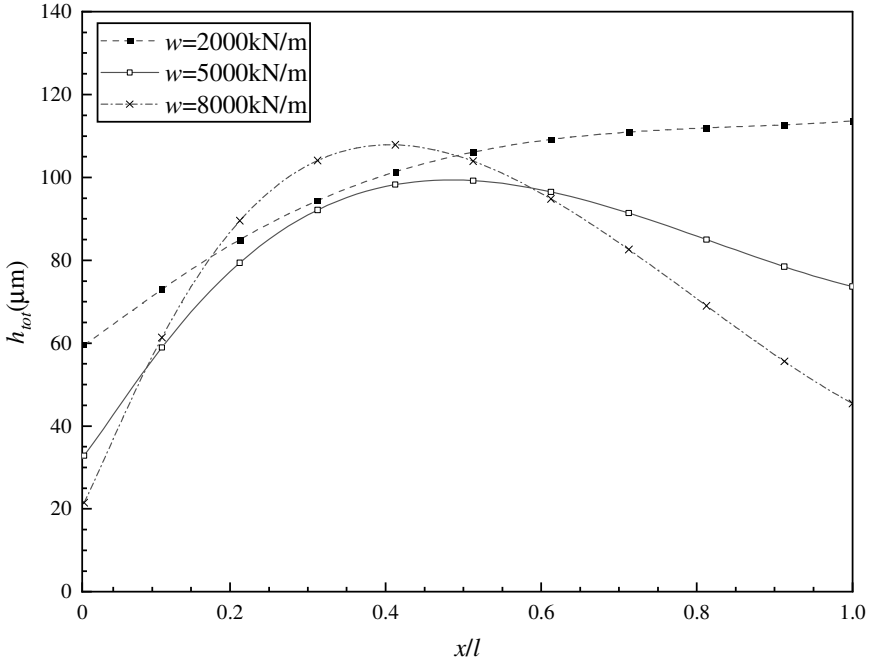

(a) *For elastically deformed surfaces without thermal deformation*

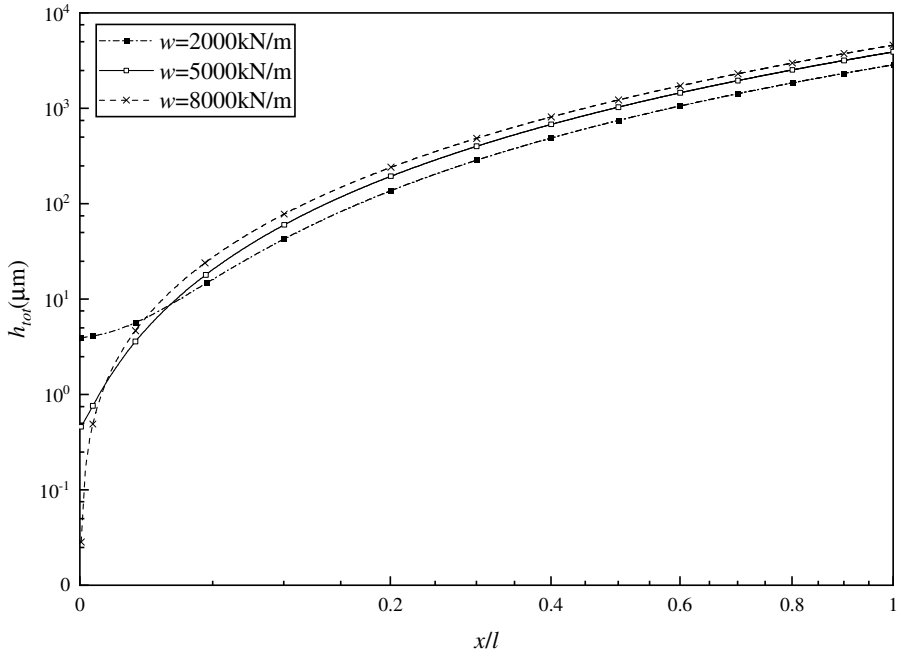

(b) *For elastically deformed surfaces with thermal deformation*

Fig. 7 *Film thickness distributions for different loads and contact regimes at u=40 m/s with medium the fluid-surface interaction*

4.3 FRICTION COEFFICIENT

Figures 8(a) and (b) show that surface thermal distortion to strongly affects the bearing friction coefficient. Due to surface thermal distortion, the friction coefficient on the stationary bush surface slightly decreases with increasing sliding speed when u exceeds 15 *m/s*, while the friction coefficient on the shaft surface increases monotonously with increasing speed. Overall, surface thermal distortion significantly reduces the bearing friction coefficient particularly at high sliding speeds.

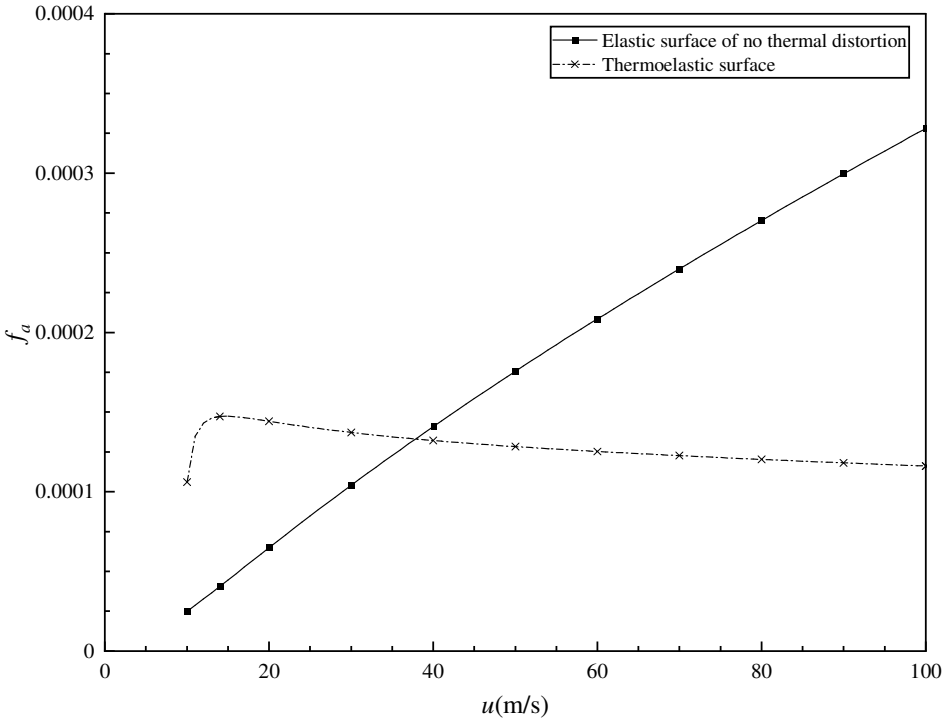

(a) *On stationary bush surface*

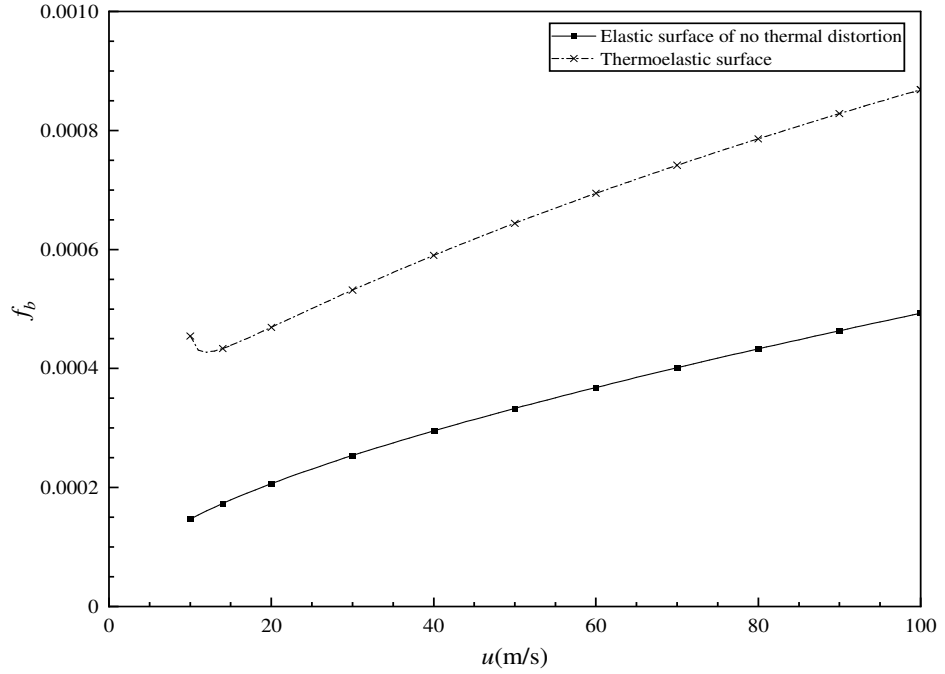

(b) *On moving shaft surface*

Fig. 8 *Friction coefficients on the stationary and moving bearing surfaces for different contact regimes at w=5000 kN/m with weak fluid-surface interaction*

5. MODEL VALIDATION

The multiscale flow model used for lubrication analysis, which incorporates the physically adsorbed molecule layer, has been validated by Jiang and Zhang [24]. The film thickness results obtained in the present study qualitatively agree with experimental observations of large hydrodynamic lubricated thrust bearing, showing film collapse due to surface thermoelastic deformation [4, 5].

6. CONCLUSIONS

The numerical computation was performed to evaluate the performance of a large hydrodynamic thrust bearing under high operational parameters, incorporating the effects of surface thermoelastic deformation and the adsorbed fluid layer. The moving shaft surface is made of steel, and the stationary bush surface is made of bronze.

Based on the obtained results, the main conclusions are as follows:

(1) For large loads and high speeds, surface thermal distortion significantly deteriorates bearing performance, resulting in substantially reduced bearing clearance. It also greatly increases the sensitivity of the minimum film thickness to load variations.

(2) For large loads and speeds, surface thermal distortion leads to a substantial reduction in the friction coefficient of the bearing.

(3) Surface thermoelastic deformation causes the bearing performance to deviate from predictions of classical hydrodynamic lubrication theory.

(4) Prior to pad seizure, strong physical adsorption of the fluid onto the bearing surface markedly improves lubrication performance.

7. REFERENCES

[1] Chambers, W.S., Mikula, A.M., Operational data for a large vertical thrust bearing in a pumped storage application, *STLE Tribology Transactions*, Vol. 31, No. 1, pp. 61–65, 1988. https://doi.org/10.1080/10402008808981798

[2] Kawaike, K., Okano, K., Furukawa, Y., Performance of a Large Thrust Bearing with Minimized Thermal Distortion, *A S L E Transactions*, Vol. 22, No. 2, pp. 125–134, 1979. https://doi.org/10.1080/05698197908982908

[3] Pajaczkowski, P., Schubert, A., Wasilczuk, M., Wodtke, M., Simulation of large thrust bearing performance at transient states, warm and cold start-up, Proceedings of the Institution of Mechanical Engineers, *Part J: Journal of Engineering Tribology*, Vol. 228, No. 1, pp. 96-103, 2013. https://doi.org/10.1177/1350650113500483

[4] LaTray, N., Kim, D., Song, M., Static Performance of a Hydrostatic Thrust Foil Bearing for Large Scale Oil-Free Turbomachines, *Journal of Engineering for Gas Turbine and Power*, Vol. 143, No. 4, 041017, 2021. https://doi.org/10.1115/1.4049884

[5] Novotny, P., Jonák, M., Jirı Vacula, M., Evolutionary optimisation of the thrust bearing considering multiple operating conditions in turbomachinery, *International Journal of Mechanical Sciences*, Vol. 195, 106240, 2021.

https://doi.org/10.1016/j.ijmecsci.2020.106240

[6] Tretiak, O., Kritskiy, D., Kobzar, I., Arefieva, M., Nazarenko, V., The methods of three-dimensional modeling of the hydrogenerator thrust bearing, *Computation*, Vol. 10, No. 9, 152, 2022. https://doi.org/10.3390/computation10090152

[7] Wang, J.L., Cao, Y., Sun, W.Y., Chen, R.L., Jia, Q., Cui, Y.H., Research on the lubrication performance of circular tilting pad thrust bearings for large wind turbines, *Lubrication Science*, Vol. 36, No. 6, pp. 421-430, 2024. https://doi.org/10.1002/ls.1681

[8] Wodtke, M., Wasilczuk, M., Performance evaluation of large-size tilting-pad thrust bearings based on results from small-size models, *Proceedings of the Institution of Mechanical Engineers, Part J: Journal of Engineering Tribology*, Vol. 239, No. 8, pp. 1064-1077, 2025. https://doi.org/10.1177/13506501251320473

[9] Lutfullaeva, A., Ali, M., Yasko, I., Fais, C., Dynamic performance evaluation of hydrodynamic tapered-land thrust bearing, *Proceedings of the Institution of Mechanical Engineers, Part J: Journal of Engineering Tribology*, Vol. 239, No. 12, pp. 1664-1681, 2025.

https://doi.org/10.1177/13506501251330107

[10] Iliev, H., Failure analysis of hydro-generator thrust bearing, *Wear*, Vol. 225, pp. 913–917, 1999. https://doi.org/10.1016/S0043-1648(98)00410-4

[11] Ettles, C.M., Size effects in tilting pad thrust bearings, *Wear*, Vol. 59, No. 1, pp. 231-245, 1980. https://doi.org/10.1016/0043-1648(80)90281-1

[12] Yuan, J.H., Medley, J.B., Ferguson, J.H., Spring-supported thrust bearings used in hydroelectric generators: Laboratory test facility, *Tribology Transactions*, Vol. 42, No. 1, pp. 126-135, 1999. https://doi.org/10.1080/10402009908982199

[13] Pinkus, O., Sternlicht, B., *Theory of hydrodynamic lubrication*, McGraw-Hill, New York, America, 1961. https://doi.org/10.1115/1.3636485

[14] Williams, P.D., Symmons, G.R., Analysis of hydrodynamic slider thrust bearings lubricated with non-newtonian fluids, *Wear*, Vol. 117, No. 1, pp. 91-102, 1987.

https://doi.org/10.1016/0043-1648(87)90246-8

[15] Singh, U.P., Mathematical analysis of effects of surface roughness on steady performance of hydrostatic thrust bearings lubricated with Rabinowitsch type fluids, *Journal of Applied Fluid Mechanics*, Vol. 13, No. 4, pp. 1339-1347, 2020.

https://doi.org/10.36884/jafm.13.04.30682

[16] Khonsari, M.M., A review of thermal effects in hydrodynamic bearings Part I: slider and thrust bearings, *STLE Tribology Transactions*, Vol. 30, No. 1, pp. 19-25, 1987.

https://doi.org/10.1080/05698198708981725

[17] Ye, X., Zhang, Y.B., Effect of surface thermoelastic deformation on the performance of the hydrodynamic big-size step bearing, *Mechanika*, Vol. 31, No. 3, pp. 211-219, 2025.

https://doi.org/10.5755/j02.mech.40713

[18] Zhang, Y.B., Modeling of flow in a very small surface separation, *Applied Mathematical Modelling*, Vol. 82, pp. 573-586, 2020. https://doi.org/10.1016/j.apm.2020.01.069

[19] Atkas, O., Aluru, N.R., A combined continuum/DSMC technique for multiscale analysis of microfluidic filters, *Journal of Computational Physics*, Vol. 178, No. 2, pp. 342-372, 2002.

https://doi.org/10.1006/jcph.2002.7030

[20] Yen, T.H., Soong, C.Y., Tzeng, P.Y., Hybrid molecular dynamics-continuum simulation for nano/mesoscale channel flows, *Microfluidics and Nanofluidics*, Vol. 3, pp. 665-675, 2007.

https://doi.org/10.1007/s10404-007-0154-7

[21] Borg, M.K., Lockerby, D.A., Reese, J.M., A multiscale method for micro/nano flows of high aspect ratio, *Journal of Computational Physics*, Vol. 233, pp. 400-413, 2013.

https://doi.org/10.1016/j.jcp.2012.09.009

[22] Zhang, Y.B., Lubrication analysis for a line contact covering from boundary lubrication to hydrodynamic lubrication: Part I- Micro contact results, *Journal of Computational and Theoretical Nanoscience*, Vol. 11, pp. 62-70, 2014.

https://doi.org/10.1166/jctn.2014.3318

[23] Zhang, Y.B., Modeling of molecularly thin film elastohydrodynamic lubrication, *Journal of the Balkan Tribological Association*, Vol. 10, No. 3, pp. 394-421, 2004.

[24] Jiang, C.T., Zhang, Y.B., Comparisons between full molecular dynamics simulation and Zhang's multiscale scheme for nanochannel flows, *Journal of Molecular Modeling*, Vol. 30, article no. 334, 2024. https://doi.org/10.1007/s00894-024-06115-8